BIOINFORMATICS ORIGINAL PAPER

Vol. 21 no. 9 2005, pages 1935–1942
doi:10.1093/bioinformatics/bti258

Gene expression

Robust estimation of protein expression ratios with lysate microarray technology

Cristian Mircean[1,2], Ilya Shmulevich[1,*], David Cogdell[1], Woonyoung Choi[1], Yu Jia[1], Ioan Tabus[2], Stanley R. Hamilton[1] and Wei Zhang[1]

[1]Department of Pathology, University of Texas M.D. Anderson Cancer Center, Houston, TX, USA and [2]Institute of Signal Processing, Tampere University of Technology, Tampere, Finland

Received on June 24, 2004; revised on December 21, 2004; accepted on December 29, 2004
Advance Access publication January 10, 2005

ABSTRACT

Motivation: The protein lysate microarray is a developing proteomic technology for measuring protein expression levels in a large number of biological samples simultaneously. A challenge for accurate quantification is the relatively narrow dynamic range associated with the commonly used chromogenic signal detection system. To facilitate accurate measurement of the relative expression levels, each sample is serially diluted and each diluted version is spotted on a nitrocellulose-coated slide in triplicate. Thus, each sample yields multiple measurements in different dynamic ranges of the detection system. This study aims to develop suitable algorithms that yield accurate representations of the relative expression levels in different samples from multiple data points.

Results: We evaluated two algorithms for estimating relative protein expression in different samples on the lysate microarray by means of a cross-validation procedure. For this purpose as well as for quality control we designed a 1440-spot lysate microarray containing 80 identical samples of purified bovine serum albumin, printed in triplicate with six 2-fold dilutions. Our analysis showed that the algorithm based on a robust least squares estimator provided the most accurate quantification of the protein lysate microarray data. We also demonstrated our methods by estimating relative expression levels of p53 and p21 in either $p53^{+/+}$ or $p53^{-/-}$ HCT116 colon cancer cells after two drug treatments and their combinations on another lysate microarray.

Availability: http://www.cs.tut.fi/~mirceanc/lysate_array_bioinformatics.htm

Contact: is@ieee.org

INTRODUCTION

Despite the enormous genomic complexity of most organisms, and in particular humans, the complexity is further increased at the protein level as a result of posttranslational modifications, such as phosphorylation, acetylation and ubiquitination, which can appreciably impact the functional state of proteins. Thus, it is not only the levels of proteins but also their modification status that will have to be studied in order to gain a deeper understanding of biological systems. A number of proteomic technologies have been developed that allow researchers to study proteins in a high-throughput fashion. Among these is the protein microarray, which may appear in different formats depending on what substrates are deposited on the solid matrix (MacBeath and Schreiber, 2000). For example, various antibodies can be spotted on the slides to produce the so-called antibody array (Ivanov *et al*., 2004).

Another format is called the reverse-phase protein lysate microarray (or simply, lysate array) where cellular lysates or purified proteins are arrayed on nitrocellulose-coated slides and probed with antibodies that recognize various proteins and their modified products (Paweletz *et al*., 2001). Several recent studies report the use of lysate arrays for investigating signal pathways using cancer specimens (Grubb *et al*., 2003; Wulfkuhle *et al*., 2003; Espina *et al*., 2003). A lysate array spotted from a library of purified proteins can also serve as a powerful tool for detecting protein–protein interactions. The advantages of a lysate array include the requirement of minimal amount of protein extracts for generation of tens of arrays, potential for automation of hybridization and considerable saving of labor compared with western blotting experiments. Another important advantage of lysate arrays over the western blotting assay is that multiple replicates and dilutions can be incorporated into the experimental design, thus making the protein level quantification more accurate. This is not insignificant because the dynamic range of commonly used protein detection methods is narrow, whereas the range of protein expression in different samples can be very large. Therefore, it is important to develop robust algorithms for analyzing the multiple data points produced by lysate arrays.

Nishizuka *et al*. (2003) profiled 60 human cancer cell lines (NCI-60) with lysate arrays using serial dilutions. After removal of outliers, dilution curves were estimated from the ten dilution points using monotonic linear spline interpolation. The patterns of protein expression were compared with those obtained for the same genes using both cDNA and oligonucleotide arrays. It was discovered that structure-related proteins exhibited a high correlation between mRNA and protein levels across the NCI-60 cell lines.

In this study, our primary objective was to develop a method for accurately estimating the relative protein expression in two different samples from a protein lysate microarray. Toward that end, we proposed and evaluated two different algorithms. For this purpose as well as for quality control we designed a 1440-spot lysate microarray containing 80 identical samples of purified bovine serum albumin (BSA), printed in triplicate with six 2-fold dilutions. We further tested the selected algorithms to quantify the expression of selected proteins in colon cancer cells after drug treatment.

*To whom correspondence should be addressed.

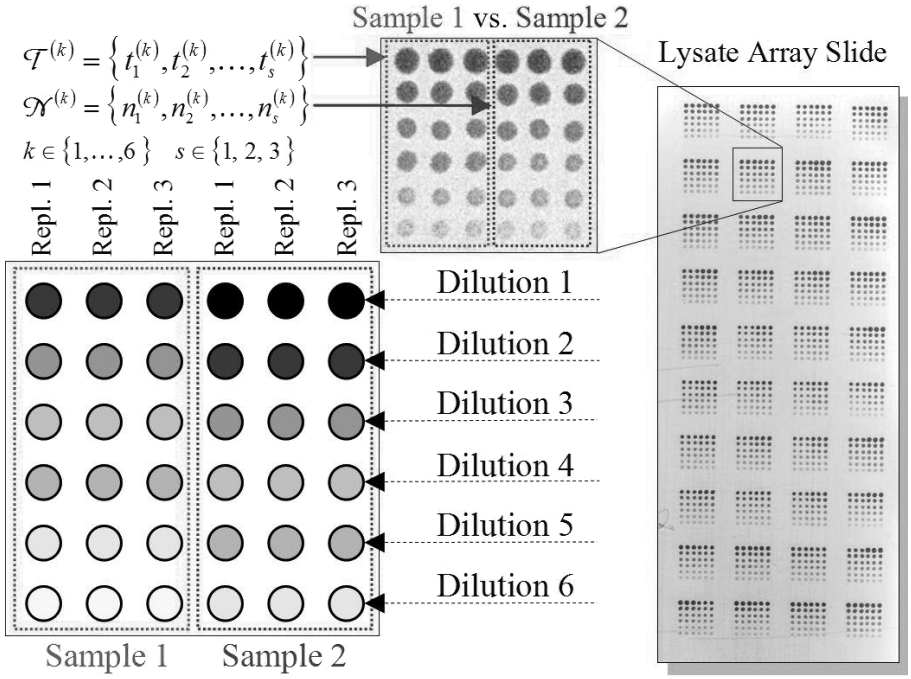

Fig. 1. The layout of the lysate arrays. The approaches proposed in this paper estimate differential protein expression. The samples are placed in patches of 18 spots, 6 dilutions and 3 replicates for each dilution, as shown in the illustration on the left. The sets $T^{(k)}$ and $N^{(k)}$ represent the measurements corresponding to two different samples (e.g. tumor and normal), with k denoting the dilution and s denoting the replicate.

MATERIALS AND METHODS

Lysate mixtures and signal detection

Cells and protein extraction Proteins were harvested from isogenic HCT116 cell lines provided by Dr Bert Vogelstein (Johns Hopkins University, Baltimore, MD). The $p53^{+/+}$ and $p53^{-/-}$ cell lines were cultured in Dulbecco's minimal essential medium (DMEM) with 10% Nu-serum (Collaborative Research Products, Bedford, MA). Lysates were collected in a buffer containing 20 mM Tris pH 7.6, 150 mM NaCl, 5 mM EDTA, 0.5% NP40 freshly supplemented with 0.02 mM leupeptin and 0.01 mM PMSF after 48 h of drug treatment at IC25. Lowry assay was used to normalize the protein concentration prior to liquid handling.

Lysate array printing BSA demonstration chips containing six 2-fold dilutions with 80 sample replicates were made by a liquid-handling robot RSP (TECAN US, Research Triangle Park, NC). These dilutions were then spotted on the nitrocellulose-coated FAST (Scheicher and Schuell, Keene, NH) or Vivid (Pall, Ann Arbor, MI) slides with 500 μm center-to-center interspot distance using a G3 spotter (Genomics Solutions, Ann Arbor, MI) to produce triplicate spots of all dilution points with the specified number of transfers. HCT116 lysate arrays were created in a similar manner with 500, 250, 125, 62.5, 31.5 and 15.625 ng/μl of protein.

Detection and imaging Detection of target protein was done by a heavily modified DAKO CSA kit (DakoCytomation, Carpinteria, CA) catalog # K1500. Briefly, the slides were blocked with reblot + Mild (Chemicon, Temecula, CA) catalog # 2502, followed by overnight blocking with i-block (Applied Biosystems, Foster City, CA) catalog # Tropix AI300. The next day, blocking continued with fresh 3% hydrogen peroxide, Avidin/Biotin and casein block. Primary antibodies p53 Ab-6 (Oncogene Research Products, San Diego, CA) and p21/WAF1 (gift from Wade Harper, Baylor College of Medicine, Houston, TX) were diluted in antibody dilution buffer and incubated at 25°C for 1 h in a humid chamber. Secondary biotinylated antibodies BA-9200 for rabbit primaries or BA-1000 for mouse primaries (Vector Laboratories, Burlingame, CA) were diluted 1:10 000 and incubated as before. Final steps included streptavidin–biotin, amplification reagent and streptavidin/peroxidase incubations from the CSA kit followed by DAB+ development. TBS–T washes preceded all steps for the removal for the previous reagent. Slides were scanned in color at 1200 DPI; the resulting image was converted to a 16-bit grayscale and inverted (negative) to allow quantification by ArrayVision™ (Imaging Research Inc.).

Design on slide and spotting

In order to tune the preprocessing stages of the liquid handling, spotting and image analysis, we created slides containing purified BSA spotted in three replicates of each sample with six 2-fold dilutions for each of 80 identical samples resulting in 1440 spots per slide. Three replicates were included to provide better error resilience and outlier detection (Fig. 1 gives the layout of the lysate microarray).

Robust estimation of expression ratios

An important goal is the estimation of the ratio between expressions of specific proteins from two samples (e.g. tumor/normal or treated/untreated). We propose and evaluate two robust approaches in comparison with standard linear regression aimed at estimating the expression ratios from lysate arrays. In an ideal case, both robust methods should yield the same results as linear regression.

In developing our approaches for estimating the protein expression ratios, our overall aim was to produce results that are biologically accurate and robust to outliers and other artifacts. We consider an outlier to be a spot that is inconsistent either with the other replicate spots in the same dilution (e.g. in a certain dilution two replicates are close to each other while the third is significantly different) or with respect to all other spots, which may be caused, e.g. by extreme saturation or a crack in the membrane affecting all spots from the same dilution.

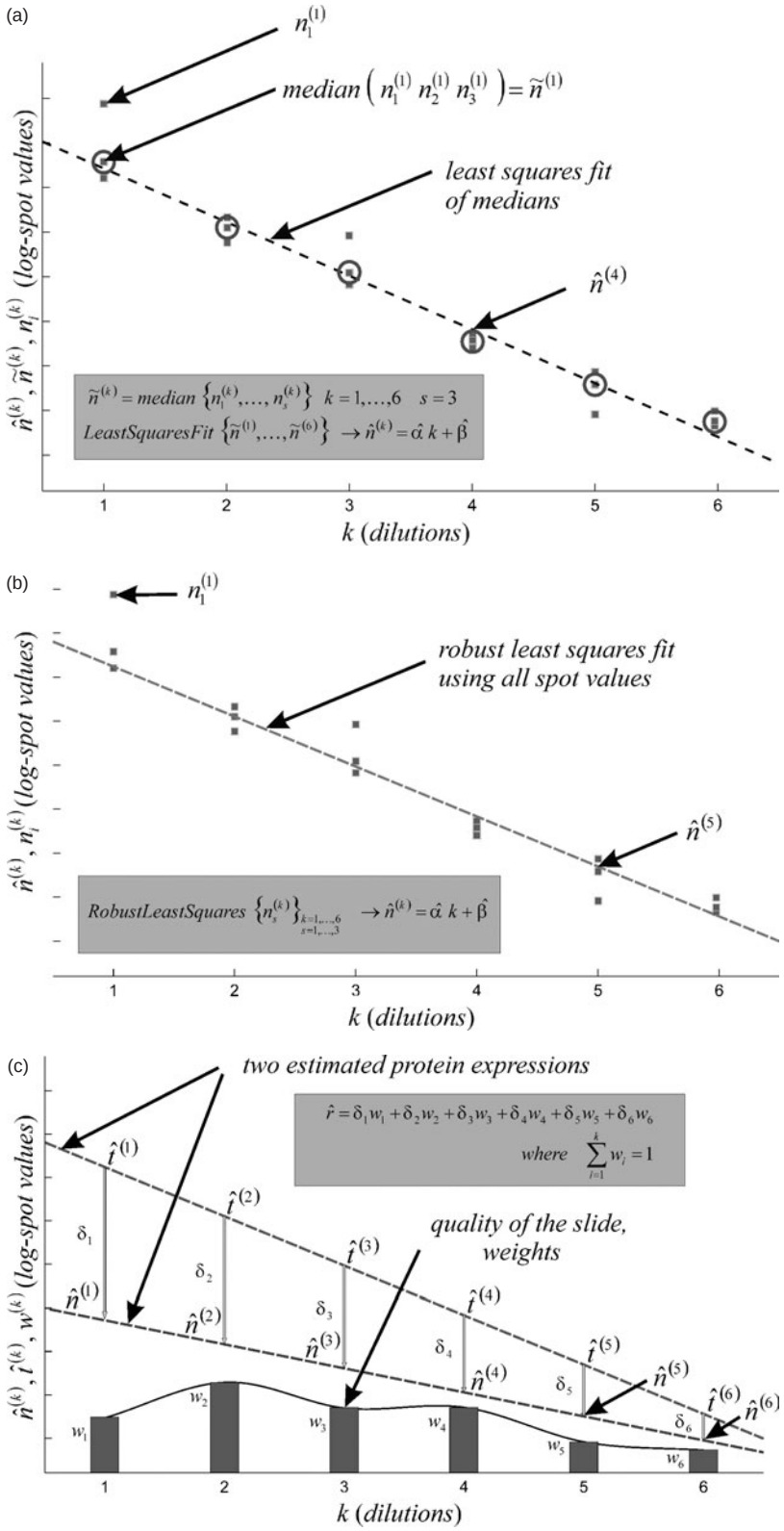

Fig. 2. Robust estimation of the protein expression ratios from six dilutions in three replicates. The model that fits the dilutions is expected to be linear in log–log space. (**a** and **b**) Graphical representation of the non-linear and robust least squares approaches, respectively (see text). (**c**) The distance between the two fitted lines at each dilution is weighted according to the estimated spot quality at that dilution (see text).

Non-linear approach The use of triplicates rather than duplicates confers an obvious advantage for robustly estimating the protein expression value. In this approach, we apply the median to the triplicates because of its outlier-resilient properties, thus providing a robust estimate of protein expression for each dilution. We then perform a least squares linear fit to the median estimated values (one estimate per dilution and sample), since the dilution is expected to be linear on a log–log scale as will become apparent in the experimental section (Fig. 5). Figure 2a illustrates the approach for the sample labeled n. The log-expression value is denoted by $n_i^{(k)}$ for the replicate i at dilution k, where $i \in \{1, 2, 3\}$ and $k = 1, \ldots, 6$; $k = 1$ corresponds to the highest concentration. For the sample labeled t, where we have the log-expression values $t_i^{(k)}$, the approach is similar. One potential drawback of the non-linear approach described here is that when all replicate spots from one dilution are erroneous, say, due to a scratch, the fitted line can be dramatically affected, even though the other dilutions may be perfectly reliable. The least squares method is optimal if the errors are normal, independent and identically distributed. However, if this is not the case, it can perform very poorly, especially if data are affected by outliers. Next, we propose a more robust method alleviating to a large extent the mentioned drawbacks.

Robust least squares This method considers all 18 spots (3 replicates, 6 dilutions) for each sample in order to fit a linear model (in log–log space). Since lysate array data may be susceptible to several artifacts such as membrane irregularities, improper spot segmentation or outliers due to saturation, that can affect all replicates for a given dilution, a robust regression scheme should be used, since one of the main disadvantages of least squares is its sensitivity to outliers. We propose the use of 'Huber' weights with an iteratively reweighted least squares algorithm that minimizes the weighted sum of squares, where the weight given to each value depends on its distance to the fitted line (Huber, 1981; Street *et al*., 1988). The algorithm, using all 18 spots from each sample, will produce a robust linear fit in log–log space. This method is shown in Figure 2b, where we use the same notation as in Figure 2a.

Estimation of protein expression ratio The distance between the two fitted lines for the two samples n and t represents the logarithm of the protein expression ratio. However, it is clear that because of experimental variability, the two lines (tumor and normal) will not be perfectly parallel. Our approach is to estimate the distances at all the six dilution points and to weight them in accordance with the estimated quality of the slide at these points. This is based on the intuition that the higher the dispersion for a particular dilution (over the entire array) the less the weight this dilution should get when calculating the distance between the two fitted lines and consequently, the less the influence this dilution should have on the final estimate of the ratio of protein expressions between the two samples. In the case of the BSA test slide, we chose the weights to be inversely proportional to the dispersion of the values for each dilution, as measured by the interquartile range. For other lysate arrays, which typically contain many different samples, we used another approach to estimate the weights by means of the coefficient of variation (CoV), which is defined as the standard deviation divided by the mean for each dilution. Specifically, for each dilution, we calculated the mean (or median) of the CoVs, where the mean is taken of the over all samples on the array, and set the weights to be inversely proportional to these values. Finally, the weights were normalized such that their sum is equal to one. In summary, we proposed the following multistage method:

(1) Fit a (robust) regression line for each sample,

(2) Calculate the dilution weights,

(3) Calculate the weighted distance between the two samples.

RESULTS AND DISCUSSION

Experiments using protein lysate arrays included multiple steps, including preparation of the biological samples, construction of lysate arrays, detection and imaging. An additional factor for lysate arrays is that when the protein concentrations from biological samples, such as microdissected cells, are very low, we want to repeat the spotting multiple times on one array in order to transfer more proteins to the lysate array. This is not normally done for cDNA microarrays and consistency of such repeated 'touches' has to be evaluated in our experiments. Quality control is crucial for the success of the experiments and for evaluation of the data analysis methods as in cDNA microarray experiments. To avoid potentially complicating factors associated with biological materials from cells, we first used a purified protein, BSA, as printing material to evaluate our lysate spotting procedures and the performance of the estimation algorithms. For example, we compared the quality of the slides after 1, 5 and 10 touches (Fig. 3), referring to the number of times a protein is transferred to the same spot on the slide by the printing robot. As seen in Figure 3, single-touch printing results in more outliers, especially in the low concentration range, but 10-touch printing

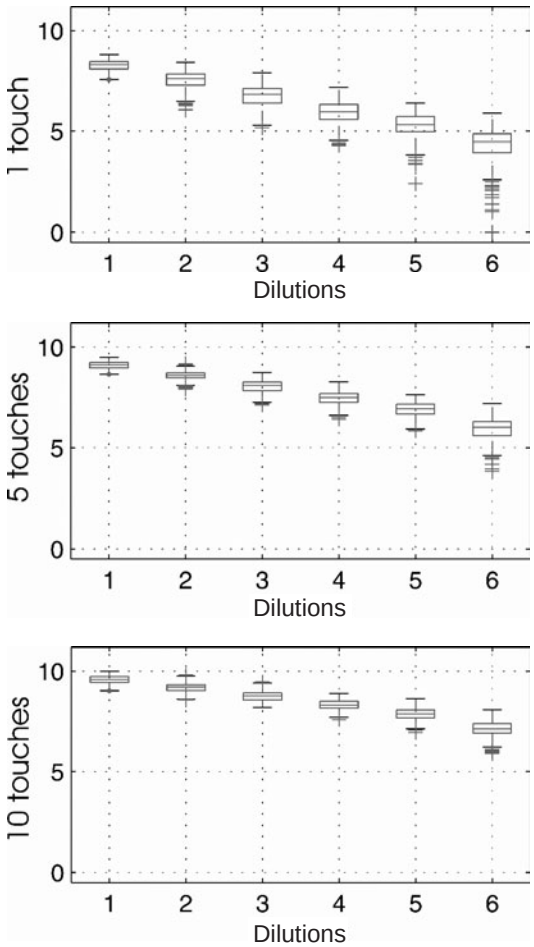

Fig. 3. A box plot showing the lower quartile, median and upper quartile values of the logarithms of the BSA spots for each of the six dilutions. The three figures, from top to bottom, compare the performance with 1, 5 and 10 touches per spot on Pall's Vivid slides. The whiskers extend to 1.5 times the interquartile range and all values beyond the whiskers are deemed to be outliers. Taking into account the number of outliers and the slope (implicitly the saturations) of the dilution curve, the best quality was obtained with 5 touches. Each boxplot represents 240 spots (80 samples × 3 replicates).

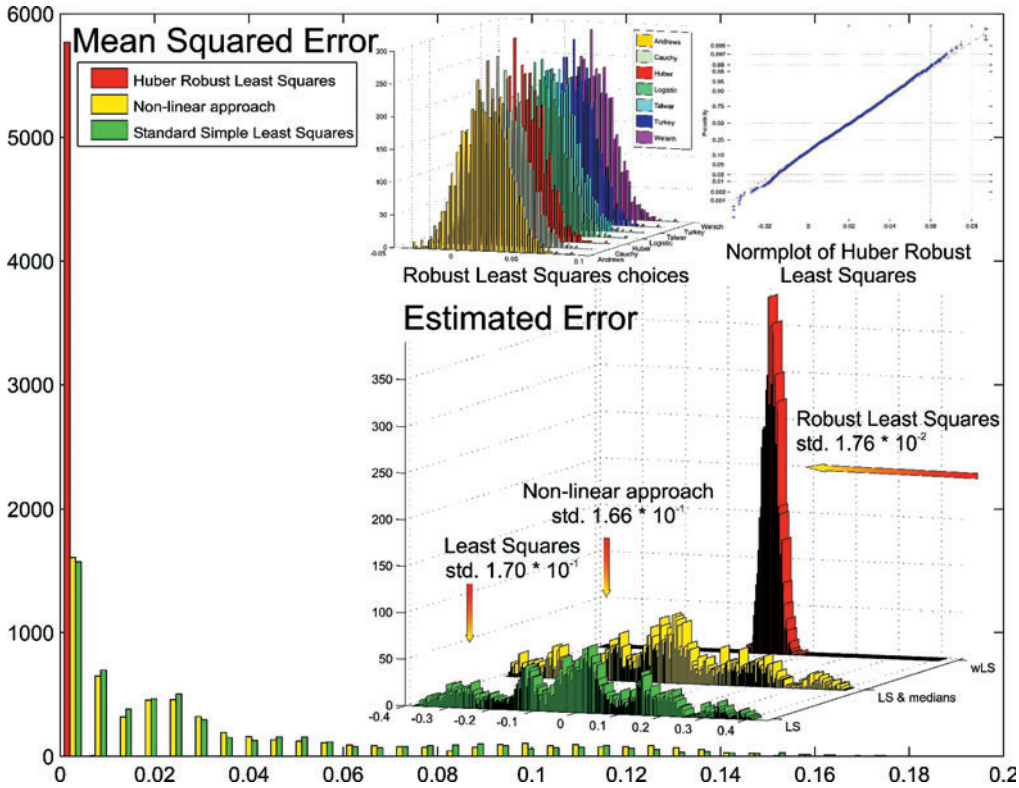

Fig. 4. Comparison of the methods using the BSA array. The main figure shows the histogram of the mean squared error (MSE) between the estimated 'true' values, computed from 49 training samples, and the estimated values computed from one test sample performed 5776 times with random splits of the data (limited by computational load). The lower inset shows the histograms of the errors for the proposed methods, defined as the difference between the estimated 'true' values and the estimated 'test' values. As can be seen, the robust least squares method that uses all 18 spots from a sample produces dramatically smaller errors than least squares applied to median estimated spot values at each dilution or than standard least squares. Additionally, the robust least squares method yields Gaussian behavior of cross-validation errors (on the split 30:49:1), as shown in the upper insets, containing the histograms of the errors as well as a normal probability plot, which is expected to appear linear for a Gaussian distribution. Standard least squares serve as a baseline comparison for either of the robust methods. For weighting procedures in robust least squares, we tested Andrews, Cauchy, Huber, Logistic, Talwar, Turkey and Welsch with similar results. Huber produced the smallest standard deviation of the mean error (std. ME). Also, other heuristic methods (not presented here) were tested with inferior results.

produces a dilution curve with an insufficiently steep slope. We found 5 touches to yield the best overall quality.

We also used the BSA array to compare the two proposed algorithms to estimate the protein expression ratios. Since all 80 samples on the BSA array are identical, under ideal circumstances, the protein expression ratios between any pair of samples should be equal to one; equivalently, the log-expression differences should be zero. Our strategy for comparing the two proposed methods with each other and with standard linear regression is based on a cross-validation approach whereby the 'true' dilution curve is estimated, by averaging from 49 samples (training set), and an error is formed between that curve and a 'test' dilution curve computed from one sample (test set). The remaining 30 samples are used for computing the weights corresponding to the quality of each dilution, as discussed earlier. The reason for reserving 30 samples for computing only the weights is to avoid computing the quality weights from the same samples to which these weights will be applied. Finally, the 49:1:30 random split is performed approximately 5700 times in order to construct the histograms of the errors (log-expression differences between the quality-weighted dilution curves). The results are shown in Figure 4. In addition to the error, we also computed the mean squared error (MSE), the histogram of which is also shown in Figure 4. Our results strongly indicate that the robust least squares approaches yield a dramatically lower error than the non-linear approach and the standard linear regression. In the iteratively reweighted least squares algorithm, there are a number of possibilities for the weight function, each protecting against outliers in slightly different ways. We used the 'Huber' weight function, but also tested other variants. Figure 4 (upper inset) shows fairly comparable results for the Andrews, Cauchy, Logistic, Talwar, Turkey and Welsch weighting schemes. Furthermore, only the robust least squares method yields cross-validation errors that are normally distributed, as shown by the histogram and the normal probability plot in Figure 4 for Huber weights.

In order to demonstrate this method in a real experimental setting, we designed another lysate array containing samples of HCT116 colon cancer cell lines under two different drug treatments (we describe them as drug 1 and drug 2) as well as a treatment consisting of a combination of the two drugs. Additionally, the array contained p53-null or $p53^{-/-}$ HCT116 cells with no treatment as well as $p53^{+/+}$ HCT116 cells (parental cells) with no treatment as a control. Each sample was spotted with six dilutions and three

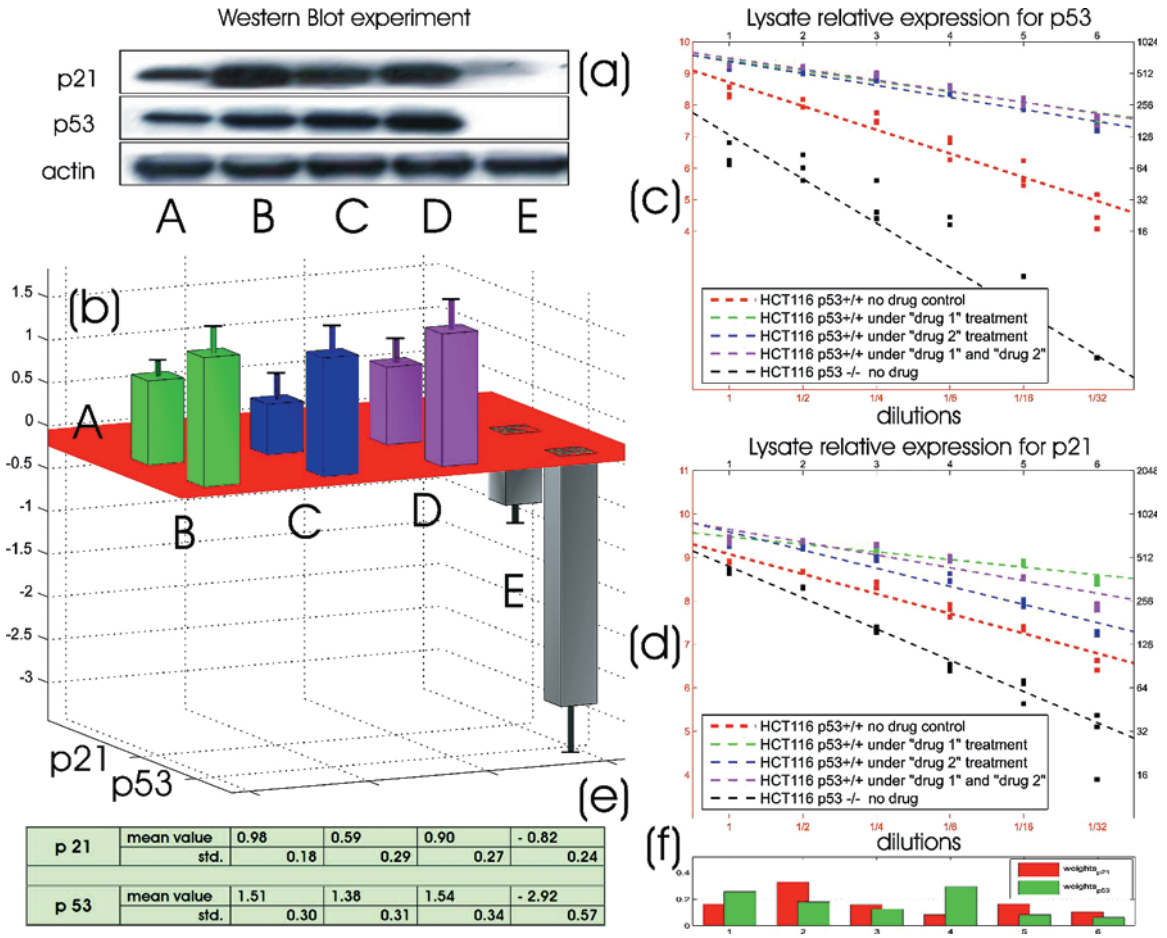

p 21	mean value	0.98	0.59	0.90	- 0.82
	std.	0.18	0.29	0.27	0.24
p 53	mean value	1.51	1.38	1.54	- 2.92
	std.	0.30	0.31	0.34	0.57

Fig. 5. Expression of p53 and p21 in $p53^{+/+}$ HCT116 cells under 'drug 1' (B), 'drug2' (C) and combination of 'drug 1' and 'drug 2' (D), as well as $p53^{-/-}$ HCT116 cells with no treatment (E), all relative to $p53^{+/+}$ HCT116 cells with no treatment (A). The no-treatment $p53^{+/+}$ HCT116 control (A) is represented as a reference baseline at zero in (**b**). The plotted bars illustrate the relative estimated values as well as the bootstrap-estimated standard deviations (1000 bootstrap samples). See the Methods section for more details. The values for the bars and standard deviations are shown in the table in (**e**). As a validation step, a western blot is shown in (**a**), with the same labels (A–E) as in (b). The quality-based weights, estimated using the coefficient of variation as described in the Methods section, are seen to be different for p21 than for p53. (**f**) shows the quality-based weights for p53 (green) and p21 (red).

replicates, as on the BSA array. Using these arrays, we measured the relative protein expressions for p53 as well as its downstream target gene product p21. All expression ratios were with respect to $p53^{+/+}$ HCT116 cells with no treatment.

To estimate the protein expression ratios, we used the robust least squares method and estimated the quality-based weights for each dilution using the mean of the coefficients of variation over the samples of the slide, as described in the Methods section. Figures 5c and d show the fitted lines for all samples, for p53 and p21, respectively.

We estimated the errors of the model once again, this time directly applied to HCT116 cells, by means of a bootstrap procedure (Efron and Tibshirani, 1993). In applying bootstrap, we have at least two different possible ways of estimating the errors for the distance between the two regressions. The two fitted lines of drug 1 (B), drug 2 (C), combination of drug 1 and drug 2 (D) and $p53^{-/-}$ no-drug (E) are compared with the expression of $p53^{+/+}$ HCT116 (A). The principles of the two methods are different. One could bootstrap the pairs $(n_i^{(k)}, k)$ and then estimate the ratio between two protein expressions as the quality-weighted distance using the bootstrap-randomized selection. Another option is to estimate the errors by means of bootstrapping the residuals.

We preferred to use the first alternative, which involves recalculation of the parameters, as it makes no assumption about whether or not the regression model holds. Figure 5b illustrates the expression ratios, relative to $p53^{+/+}$ HCT116 cells with no treatment, indicated as a baseline at zero, along with the bootstrap-estimated standard deviations. Because the bar graphs in Figure 5b represent distances, the standard deviations on these bars incorporate the combined variability owing to the treatment (or $p53^{-/-}$) and the $p53^{+/+}$ no-drug reference.

As expected, the $p53^{-/-}$ cells (E) have a much lower p53 relative expression than all other conditions. The same behavior is seen for p21 expression, but not so dramatically. Further, the combination of drugs (D) does not increase the expression of p53 and p21 in HCT116 $p53^{+/+}$ cells, relative to drug 1 (B) or drug 2 (C) alone. As a validation step, Figure 5a shows a western blot corresponding to all tested conditions.

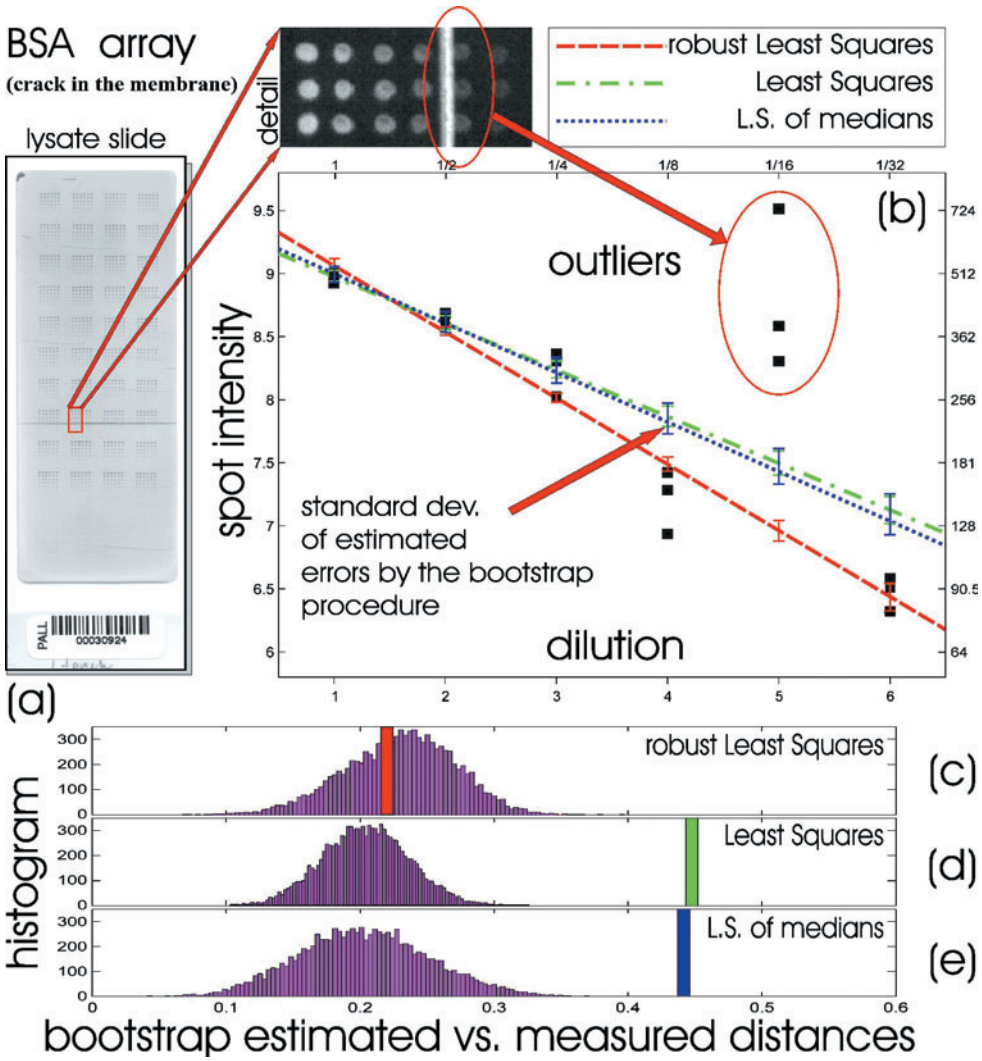

Fig. 6. To study the robustness of the algorithms, the three methods were applied on a BSA array with a crack in the membrane. The sample 59 is presented in the original slide image (**a**) and then before quantifying in a negative image prepared for ArrayVision™. As result, all three replicates of the fifth dilution are outliers (**b**). The simple linear regression is most affected by this error, followed by the 'non-linear approach' robust least squares is able to reject the effect of outliers. Furthermore, using a bootstrap procedure (1000 times), which combines the pairs of spot intensity and dilution (see Discussion section), the estimated errors from robust least squares are considerably lower than from the other two cases. The error bars on the fitted lines represent the standard deviations of the estimated fits for each dilution using the bootstrap procedure. The lower inset shows bootstrap histograms (10 000 bootstrap samples) of distances between two neighboring normal samples, computed with robust least squares (**c**), least squares (**d**) and least squares of the medians (**e**). In each subplot, the vertical bar indicates the distance between a 'cracked' sample and its neighboring normal sample, using the same algorithm that is used to generate the histogram.

The HCT116 cell data are fairly free of outliers. In an ideal case, the two robust methods should return the same results as a standard regression model. We considered it fit to report the case, where the three methods return significantly different results, a case not used in our further analyses. The slide in question is spotted with BSA, with 1-touch. We can observe several cracks of the membrane caused by erroneous handling combined with a faster drying on a Pall's Vivid slide. On the left of Figure 6, we show the entire slide. The upper detail is the processed image as described in the Methods section, before applying the segmentation step of ArrayVision™. For this sample, the values of the fifth dilution spots are strongly affected by the crack and, as we can see, in reality the spots themselves are not outliers. From the three models, we can observe the robust least squares to be the least influenced, followed by least squares of the medians method (non-linear approach), and finally by standard least squares. Further it may be useful, as an additional step, to conduct a test of linearity (on the log-scale) prior to applying any of the aforementioned methods (Neter *et al*., 2004).

In measuring the expression of samples, an important question is to determine if the sample is significantly different from another. The results of the three algorithms are compared on the cracked membrane sample and two normal samples. In Figure 6, we plot bootstrap histograms (10 000 runs, resampling with replacement was performed separately for each dilution) of the distances between two neighboring normal samples, using each of the three estimation methods. The distance between the sample influenced by the

cracked membrane and the neighboring normal sample is in the same range (*P*-value 0.61) using the robust least squares method (Fig. 6c), in contrast to the other two algorithms (*P*-value is zero) (Fig. 6d and e). The distances between the 'cracked' and 'normal' samples are shown by the bars in Figure 6c, d and e.

Our quality control experiments and evaluation of several proposed methods for estimating the relative protein expressions, using a specially designed BSA array, indicate that this technology, coupled with the computational methods described here, can be used to robustly determine protein differential expression in a high-throughput manner. The experiments with HCT116 cells further support this claim. We demonstrate that the robust least squares approach provides an accurate quantification for protein lysate arrays that contain multiple data points for each sample.

ACKNOWLEDGEMENTS

The work was partially supported by the Tobacco Settlement Fund to M.D. Anderson Cancer Center (MDACC) as appropriated by the Texas Legislature, a grant from Kadoorie Foundation to MDACC, a grant from the Goodwin Fund and the Cancer Center Supporting Grant from NIH/NCI, and a grant from the Academy of Finland.

REFERENCES

Efron,B. and Tibshirani,R.J. (1993) *An Introduction to the Bootstrap*. Chapman and Hall, New York.

Espina,V., Mehta,A.I., Winters,M.E., Calvert,V., Wulfkuhle,J., Petricoin,E.F.,III and Liotta,L.A. (2003) Protein microarrays: molecular profiling technologies for clinical specimens. *Proteomics*, **11**, 2091–2100.

Grubb,R.L., Calvert,V.S., Wulkuhle,J.D., Paweletz,C.P., Linehan,W.M., Phillips,J.L., Chuaqui,R., Valasco,A., Gillespie,J., Emmert-Buck,M., Liotta,L.A. and Petricoin,E.F. (2003) Signal pathway profiling of prostate cancer using reverse phase protein arrays. *Proteomics*, **11**, 2142–2146.

Huber,P.J. (1981) *Robust Statistics*. Wiley, New York.

Ivanov,S.S., Chung,A.S., Yuan,P.Z., Guan,A.Y., Sachs,K.V., Reichner,J.S. and Chin,Y.E. (2004) Antibodies immobilized as arrays to profile protein post-translational modifications in mammalian cells. *Mol. Cell Proteomics*, **8**, 788–795.

MacBeath,G. and Schreiber,S.L. (2000) Printing proteins as microarrays for high-throughput function determination. *Science*, **289**, 1760–1763.

Neter,J., Kutner,M.H., Wasserman,W. and Nachtsheim,C.J. (2004) *Applied Linear Regression Models with Student CD-rom*, 4th edn. WCB/McGraw-Hill, Boston, New York.

Nishizuka,S., Charboneau,L., Young,L., Major,S., Reinhold,W.C., Waltham,M., Kouros-Mehr,H., Bussey,K.J., Lee,J.K., Espina,V. *et al*. (2003) Proteomic profiling of the NCI-60 cancer cell lines using new high-density reverse-phase lysate microarrays. *Proc. Natl Acad. Sci. USA*, **24**, 14229–14234.

Paweletz,C.P., Charboneau,L., Bichsel,V.E., Simone,N.L., Chen,T., Gillespie,J.W., Emmert-Buck,M.R., Roth,M.J., Petricoin,E.F. III and Liotta,L.A. (2001) Reverse phase protein microarrays which capture disease progression show activation of pro-survival pathways at the cancer invasion front. *Oncogene*, **20**, 1981–1989.

Street,J.O., Carroll,R.J. and Ruppert,D. (1988) A note on computing robust regression estimates via iteratively re-weighted least squares. *Am. Stat.*, **42**, 152–154.

Wulfkuhle,J.D., Aquino,J.A., Calvert,V.S., Fishman,D.A., Coukos,G., Liotta,L.A. and Petricoin,E.F. III (2003) Signal pathway profiling of ovarian cancer from human tissue specimens using reverse-phase protein microarrays. *Proteomics* **3**(11), 2085–2090.